ACS OMEGA

Open Access

http://pubs.acs.org/journal/acsodf

Article

Adsorption Study of Neodymium from the Aqueous Phase Using Fabricated Magnetic Chitosan-Functionalized Graphene Oxide Composites

Asmaa S. Al-salem,* AbdEIAziz A. Nayl,* Mutairah S. Alshammari, and Ismail M Ahmed

Cite This: *ACS Omega* 2024, 9, 32175−32184

Read Online

ACCESS | Metrics & More | Article Recommendations

ABSTRACT: This work reports the performances of the magnetic chitosan@graphene oxide composite (MCh@GO) for the sorption of Nd(III) from aqueous medium. The prepared composite was synthesized by a coprecipitation method and then examined by FT-IR, XRD, SEM, and TGA. XRD analysis proved physical interactions between magnetic chitosan and graphene oxide through (inter- and intramolecular H-bonding and peptide bonding). TGA data approved the thermal stability of the prepared MCh@GO nanocomposite over their constituents. The optimum pH for the sorption process was 4.5. The Langmuir model and PSO fitted the experimental data. The adsorption process was found to be endothermic and spontaneous with a Q_{max} of 56.6 mg g^{-1}. Indeed, the MCh@GO composite proved to be an excellent adsorbent for the purification, remediation, and separation of Nd due to its promising properties.

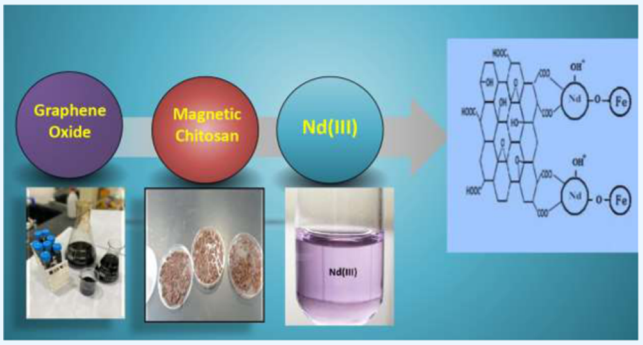

1. INTRODUCTION

Neodymium (Nd), a light rare-earth element (REE), has an abundance of 33−41 ppm in the Earth's crust. Its unique properties make it highly valuable in new and high-technology materials such as in the manufacturing of powerful permanent magnets, electronics, and renewable energy technologies. However, the limited availability and rising demand for neodymium have led to increased efforts to recover this metal from both primary and secondary sources. These recovery processes conserve the resources and protect the environment from solid wastes and wastewater effluents containing Nd and lessen adverse environmental consequences.[1,2] In this context, different techniques have been developed to recover Nd from aqueous media such as solvent extraction,[3−8] reverse osmosis,[9] coagulation and flocculation,[10−13] membrane separation,[14] and ion exchange.[15] Several of these techniques have drawbacks, including high costs, significant energy consumption, and potential inefficiency in complex matrices, particularly at trace levels. Adsorption is considered beneficial because of its reversibility, simplicity, environmental friendliness, economics, efficiency, availability of a number of adsorbents, regeneration and reuse of the sorbent used, and cleaner technique that may be applied on a large scale in the treatment processes.[16,17] However, there are drawbacks in the filtration and regeneration of adsorbents, which attract attention to modify the used sorbents by many ways like the use of magnetic materials and bridging with other sorbents that have a large surface area to overcome the above difficulties and make the solid−liquid separation easy and rapid, without centrifugation or filtration.

Some effective adsorbent materials were extensively investigated such as graphene oxide (GO)-based nanomaterials that have unique characteristics with a large specific surface area and various oxygenated functional groups such as carbonyl, carboxyl, hydroxyl, and epoxy groups.[18] Also, the 2D plane structure of graphene enhances their ability to adsorb metals ions,[19,20] but the self-agglomeration limits their use. On the other hand, chitosan (CS) is a natural polyaminosaccharide and is the most abundant biopolymer in nature after cellulose, where it has amino (NH_2) and hydroxyl (OH) groups in its molecular structure contributions, which act as the active sites.[21,22] However, chitosan also has some drawbacks such as its swelling ability, limited applications in neutral and basic media due to the deprotonation of the amino group, and slow kinetic rate. Hence, modification of GO and chitosan was investigated by many authors for the recovery of REEs and neodymium in particular.[23−28] Insertion of magnetite to the

Received: May 19, 2024
Revised: July 1, 2024
Accepted: July 3, 2024
Published: July 15, 2024

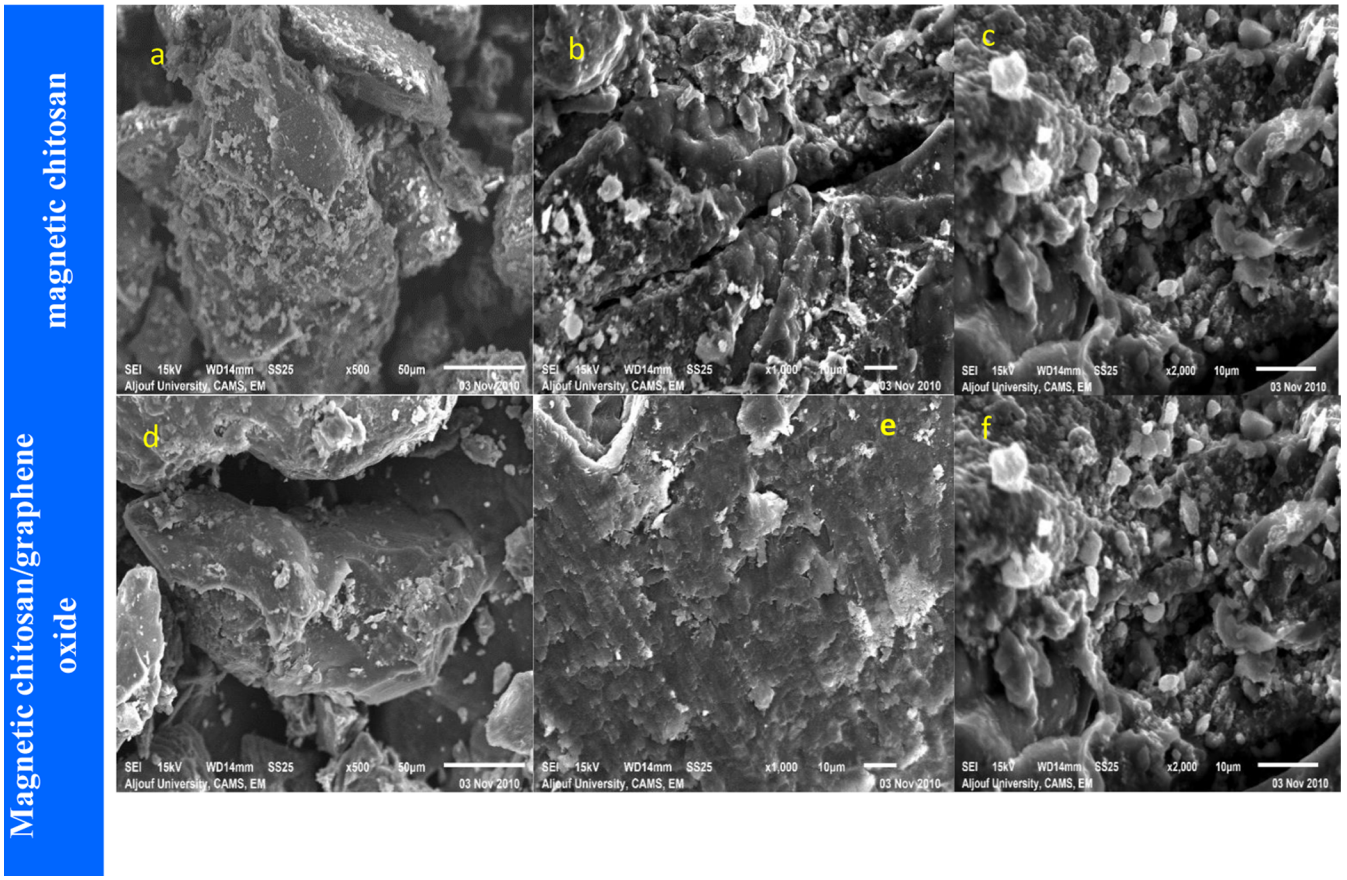

Figure 1. Images of SEM of the magnetic chitosan [a, b, c] and magnetic chitosan/graphene oxide (MCh@GO) [d, e, f] with magnifications of 500×, 1000×, and 2000×, respectively.

GO and CS molecules was done to facilitate the recovery of the composite from aqueous media. The magnetic chitosan@graphene oxide composite (MCh@GO) was really investigated by many authors for the sorption of heavy metals such as Ni^{2+}, Zn^{2+}, Co^{2+}, Pb^{2+}, Hg^{2+}, Cu^{2+}, and Cr(VI) in addition to the remediation of dyes.[29−33] However, to the best of our knowledge and based on the literature, this composite was not used for the sorption of Nd(III). Therefore, the aim of work was directed toward preparing and characterizing the prepared magnetic chitosan@graphene oxide composite (MCh@GO) and investigating the adsorption performance of the prepared composite to adsorb Nd(III). The prepared MCh@GO nanocomposite was characterized by various techniques such as (SEM), (FTIR), (XRD), and (TGA). Also, different parameters affecting the adsorption processes were studied. The obtained results were analyzed with isothermal, kinetic, and thermodynamic models to better investigate the mechanisms driving the excellent adsorption performance of Nd(III) onto MCh@GO. Finally, the regeneration and reuse of MCh@GO can be done easily.

2. METHODS AND MATERIALS

2.1. Chemicals and Materials. All chemicals were analytical grade and were purchased from Sigma-Aldrich; no further purification was required.

2.2. Preparation of Graphene Oxide, Magnetite, and Magnetic Chitosan. Graphene oxide (GO) was synthesized as reported in Hummer's method.[34] Also, magnetite was prepared using $FeCl_3$ and $FeCl_2.2H_2O$ with a ratio of 2:1 in a three-necked flask and purged with N_2 gas for 30 min at 70 °C, as reported by Lian et al.[35] Magnetic chitosan (MCh) was synthesized by adding 3.0 g of chitosan (Ch) in a mixture of 300 mL of double-distilled water (DDW), 9.0 mL of acetic acid, and 20 mL of glutaraldehyde. The mixture was stirred continuously for 2.0 h at 60 °C. The remaining residue was washed with petroleum ether, ethanol, and then DDW (in the same sequence) until removing acetic acid odor and reaching pH 7.0. The residue was oven-dried at 50 °C.

2.3. Preparation of Magnetic Chitosan@Graphene Oxide. To prepare MCh@GO, 2.0 g of MCh was added to 0.5 g of GO in 4:1 ratio of MCh@GO or 20% GO and 80% MCh and the mixture was mixed in 200 to 250 mL of DDW and then sonicated for 1.0 h at 60 °C and pH 7.0.[36] The mixture is filtered, and the precipitate was washed thoroughly with 2% NaOH. The resulting precipitate was stored in the oven at 60 °C overnight.

2.4. Instrumentations. In this study, various techniques were used to characterize the synthetic compounds GO, MCh, and (MCh@GO) nanocomposite. FTIR of the prepared composite before and after sorption was examined in the region of 400−4000 cm^{-1} using a Shimadzu IRTracer-FTIR (Shimadzu, Japan). XRD measurements of GO and MCh@GO samples were performed with bands within 2θ (10−80°) using an X-ray diffractometer (XRD 7000 maxima, Shimadzu, Japan). The surface morphology of the prepared compounds (MCh@GO and MCh) was obtained by SEM at different magnifications from 100 to 5000 using a Thermo Scientific Quattro ESEM, USA. The thermal behavior of the MCh@GO

https://doi.org/10.1021/acsomega.4c04742
ACS Omega 2024, 9, 32175−32184

was examined using a TGA-51A Shimadzu, Japan. The concentration of Nd(III) was measured spectrophotometrically using the arsenazo(III) method.[37]

The removal percentage (%**R**) is calculated by the equation

$$\%\mathbf{R} = \frac{(C_i - C_f)}{C_i} \times \mathbf{100} \quad (1)$$

where C_i and C_f are the initial and equilibrium concentrations of neodymium(III) ions, respectively (mg/L).

2.5. Adsorption of Nd(III) onto MCh@GO. Generally, 0.02 g of the composite was shaken with 10.0 mL of Nd(III) ions in the pH range (2.0−5.0). The concentration of Nd(III) was investigated in the range of 50.0−350 ppm, while the influence of temperature was examined in the range of 25−60 °C within 1.0−30.0 min stirring time, unless otherwise stated.

3. RESULTS AND DISCUSSION

Generally, GO is a nontoxic, environmentally friendly, low-cost material with a large surface area containing oxygenated groups (hydroxyl, epoxy, and carboxyl). On the other hand, chitosan is one of the emerging materials for various applications. The most intensive studies have focused on its use as a biomaterial and for biomedical, cosmetic, and packaging systems. Chitosan

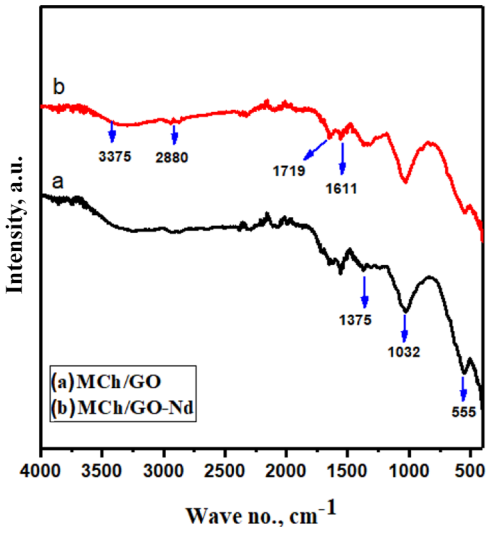

Figure 2. FTIR spectra of the MCh@GO nanocomposite before and after sorption.

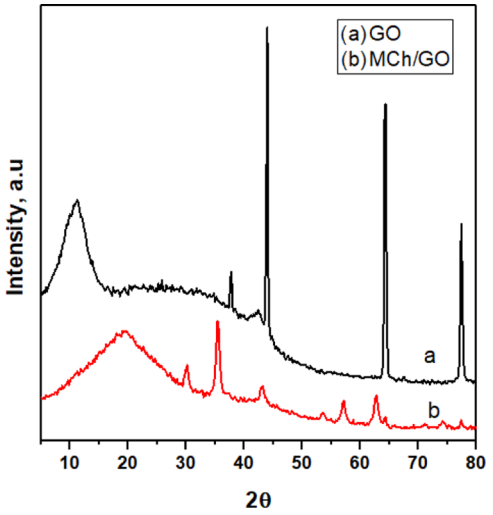

Figure 3. XRD for GO, magnetic chitosan, and the MCh@GO nanocomposite.

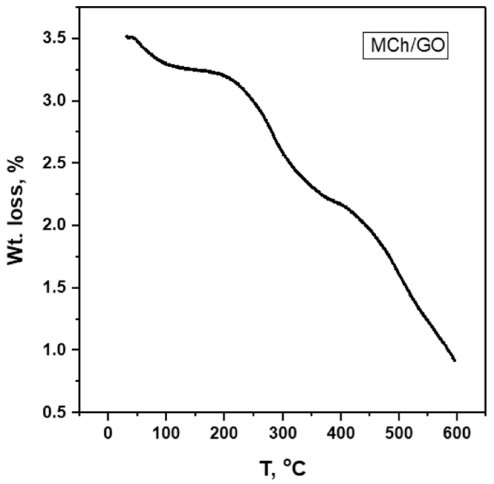

Figure 4. TGA of the MCh@GO nanocomposite.

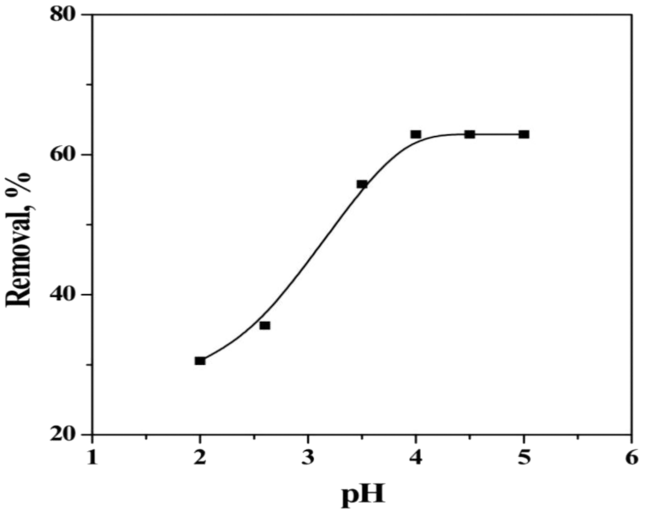

Figure 5. Effect of pH on the adsorption of Nd(III) onto the MCh@GO nanocomposite (T = 25 $C°$, V/m = 1000 mL/g, Nd(III) = 50 ppm).

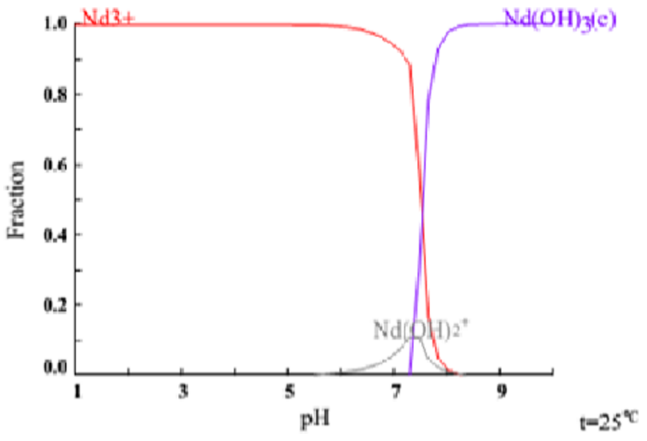

Figure 6. Distribution of the complexes formed in the aqueous phase at different pH values.

https://doi.org/10.1021/acsomega.4c04742
ACS Omega 2024, 9, 32175−32184

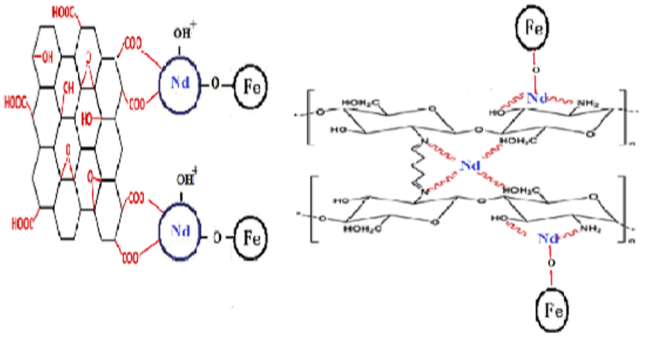

Figure 7. Proposed interaction between the MCh@GO nanocomposite and Nd(III) species.

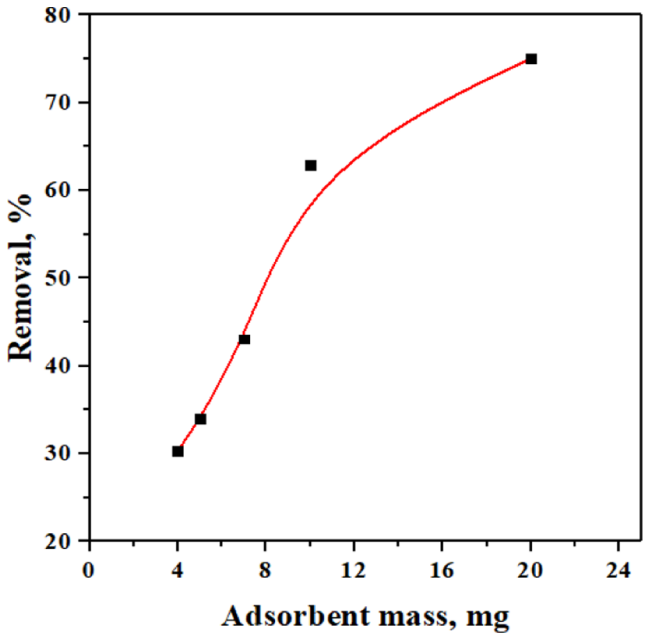

Figure 8. Effect of the mass of adsorbents on the adsorption of Nd(III) onto the MCh@GO nanocomposite. (pH = 4.5, T = 25 °C, [Nd(III)] = 50.0 ppm).

and its derivatives have received much attention in the food industry, mainly for its antimicrobial and antioxidant properties.[38−41] Therefore, the synthesized composite investigated in this work is believed to be safe.

3.1. Characterization of the Synthesized Composites.

The synthesized magnetic chitosan@graphene oxide (MCh@GO) nanocomposites were characterized by various techniques such as SEM, FTIR, XRD, and TGA.

The surface morphologies for the prepared nanocomposites can be illustrated in the SEM images. SEM images of the prepared magnetic chitosan (MCh); Figures 1a−c shows much more irregular, rough-textured surfaces than those of the chitosan films that are usually smooth and form a porous supporting framework. White crystals of magnetite (Fe_3O_4) deposited on the chitosan surface. The magnetic nanoparticles on the prepared composite also (see SEM images) illustrate that the surface of magnetic chitosan has many cavities that improve the adsorption processes. On the other hand, Figure 1d−f represents the surface morphology of magnetic chitosan@graphene oxide (MCh@GO) nanocomposite and reveals the nonhomogeneous and rough surfaces. Also, high-magnification SEM images exhibit polar surface groups,

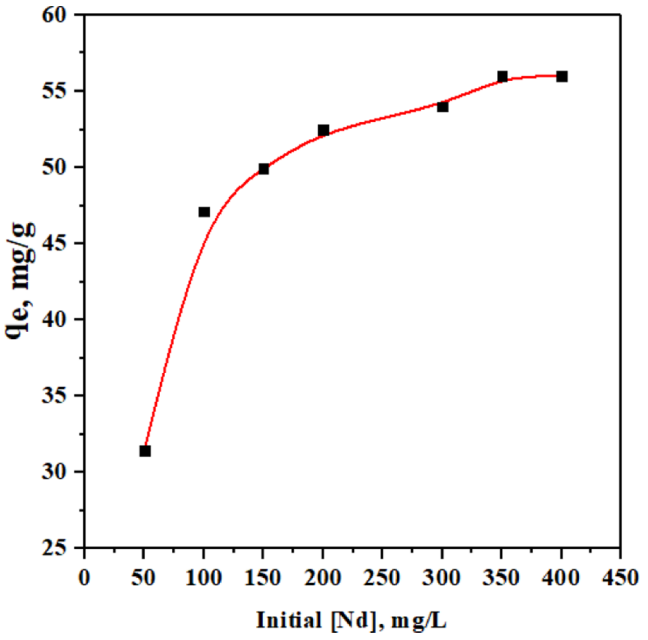

Figure 9. Effect of initial concentration on adsorption of Nd(III) onto the MCh@GO nanocomposite (pH = 4.5, T = 25 °C, V/m = 1000 mL/g).

showed by shiny and rigidly smooth morphologies with crumbled-like surfaces without the obvious white crystals that appear, revealing that magnetic chitosan particles have been assembled onto graphene oxide layers.[20,42,43]

FTIR was utilized to observe the change in surface functional groups and the structural characterizations of the fabricated nanocomposites. The FTIR pattern of magnetic chitosan and MCh@GO nanocomposite displayed in Figure 2 showed the characteristic bands for GO at 3375, 1611, and 1719 cm^{-1}, attributed to the presence of −OH stretching, −C═C− skeletal, and −C−O− stretching vibrations, respectively.[44−46] The bands at 2880, 1375, and 1032 cm^{-1} are attributed to the presence of CH_2, C−OH, and C−O−C stretching, respectively, while the band at about 555 cm^{-1} is observed due to the vibration of the Fe−O bond.[45,47] A reduction in the intensity of OH and C−OH bond stretching after the interaction with Nd is easily observed.

The crystalline structures of the synthesized nanocomposites were investigated using XRD. Figure 3 illustrates the XRD pattern of GO and the MCh@GO nanocomposite. The diffraction pattern of GO shows two characteristic peaks at $2\theta \approx 11.3°$ that refers to the (001) crystal plane of GO also at $2\theta \approx 43.9°$.[44,48,49] The diffraction pattern of magnetite exhibits peaks at $2\theta \approx 30.4$, 35.8, 43.4, 53.8, 57.4, and 63.0°, illustrating the high crystalline nature of magnetite nanoparticles, and these results approve the presence of these nanoparticles in the pure cubic forms.[49] A broad peak at $2\theta \approx 18.9°$ showed the amorphous structure of the MCh@GO nanocomposite.[45,50]

The thermal stability of the fabricated nanocomposites was determined by thermogravimetric analysis (TGA). Figure 4 represents TGA experimental results characterized to study the compositions and thermal stabilities of the MCh@GO nanocomposite that exhibits three degradation steps in this range. The first weight loss step occurs at about 30−100 °C due to the liberation of H_2O molecules on the polymer chain.[51,52] In the second step, eliminations of oxygenated functional groups of graphene oxide (such as −C═O, −C−

https://doi.org/10.1021/acsomega.4c04742
ACS Omega 2024, 9, 32175−32184

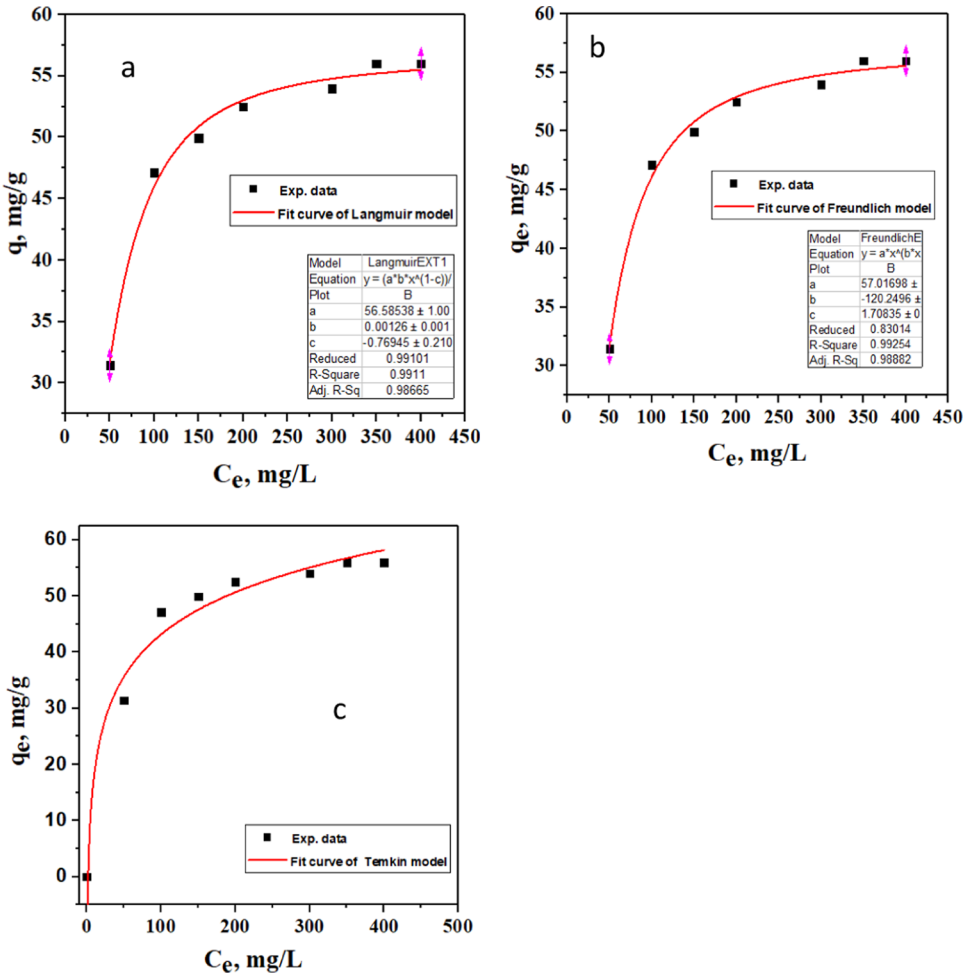

Figure 10. (a) Langmuir, (b) Freundlich, and (c) Temkin plots for the adsorption of Nd(III) onto the MCh@GO nanocomposite (pH = 4.5, T = 25 C°, V/m = 1000 mL/g).

Table 1. Langmuir and Freundlich Constants for Nd(III) Adsorption onto the MCh@GO Nanocomposite

model	parameters	value
Langmuir	Q_{max}(mg/g)	56.60
	b(L/g)	0.067
	R_L	0.229
	R^2	0.991
Freundlich	$1/n$	0.191
	K_f (mg/g)(L/mg)$^{1/n}$	19.770
	R^2	0.882
Temkin	B(J/mol)	301.85
	K_T (L/g)	3.655
	R^2	0.915

O−C, and −OH) and decomposition of polysaccharide structures occur in the range of 220−320 °C. The last decomposition step was observed at 320−600 °C due to the loss of remaining weight of chitosan with no residual mass left, which indicates full decomposition of the chitosan.[47,53]

3.2. Adsorption of Neodymium [Nd(III)]. Adsorption performance of neodymium (Nd(III)) onto the MCh@GO nanocomposite was investigated under different factors such as the effect of pH, adsorbent dose, Nd(III) concentration, and temperature.

3.2.1. Effect of pH. pH is a vital parameter affecting the sorption process and the nature of the adsorbent and adsorbate. The influence of pH on the removal of 50 mg/L Nd(III) by the MCh@GO nanocomposite was examined between 2.0 and 5.0 at ambient temperature, V/m = 1000 mL/g, and an equilibration time of 5.0 min, Figure 5. The sorption increases with increasing pH value up to 4.0 and then becomes constant. The limited uptake at low pH value could be referred to electrostatic repulsion between the metal ion and the protonated amino groups in the chitosan; it is worth mentioning that the point of zero charge of the MCh@GO nanocomposite was about 7.9.[54]

Speciation of 50 mg/L Nd(III) ions in the pH range of 1.0−12 at room temperature and an ionic strength of 0.01 was performed using the MEDUSA program[55] and is illustrated in Figure 6. The proposed interaction between the MCh@GO nanocomposite and Nd(III) species is illustrated in Figure 7. Indeed, in this work, all experiments were carried out at pH 4.5.

3.2.2. Effect of the Adsorbent Dose. The influence of the MCh@GO nanocomposite dose on the removal percentage of Nd(III) was investigated in the range of 4.0−30.0 mg at pH 4.5, illustrated in Figure 8. The sorption was found to increase sharply by increasing the MCh@GO dose at optimum conditions up to 20 mg and then became almost constant due to agglomeration of the active solid phase at a higher

https://doi.org/10.1021/acsomega.4c04742
ACS Omega 2024, 9, 32175−32184

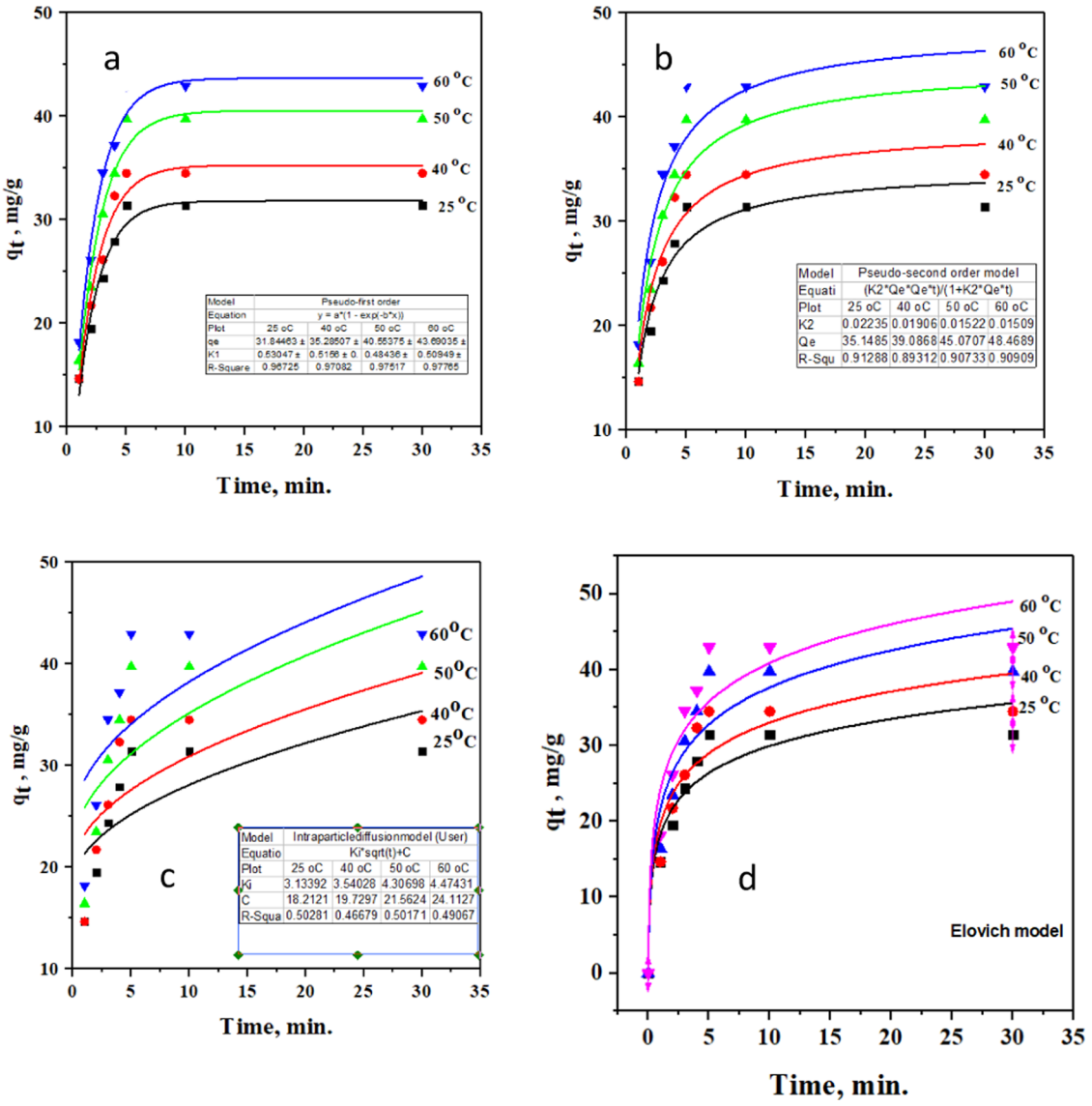

Figure 11. (a) Pseudo-first order model, (b) pseudo-second-order model, (c) intraparticle diffusion kinetic model, and (d) Elovich kinetic models for the adsorption of Nd(III) onto the MCh@GO nanocomposite (pH = 4.5, V/m = 1000 mL/g, Nd(II) = 50 ppm).

dose.[56] Therefore, 20 mg, i.e V/m = 1000 mL/g, was chosen as the dose in further investigations.

3.2.3. Effect of Nd(III) Concentration. The effect of the initial concentration of Nd(III) solutions on its sorption onto the MCh@GO nanocomposite was discussed in the range 50−350 mg/L, Figure 9. The amount adsorbed (q) slightly increased with the initial Nd(III) concentration. This is in regard to the fact that at low concentrations of Nd(III), the number of Nd(III) ions is low compared with the sufficient active sorption sites of the adsorbent. Then, it becomes almost saturated with increasing initial concentration as there are no active MCh@GO nanocomposite sites sufficiently available.[57]

In this study, the adsorption behavior of Nd(III) onto the MCh@GO nanocomposite from aqueous media was analyzed by fitting the sorption isotherm data for the adsorption of Nd(III) at various concentrations by different isotherm models (Langmuir, Freundlich, and Temkin models), eqs 2−4

$$q_e = \left(\frac{q_{max} b C_e}{1 + bC_e}\right) \quad (2)$$

$$q_e = k_f C_e^{1/n} \quad (3)$$

where q_e is the amount adsorbed (mg/g), C_e is the equilibrium concentration of the metal ion (mg/L), b is the Langmuir constant, and K_f and n are the Freundlich constants. The results are illustrated in Figure 10a,b and Table 1. It is clear that the Langmuir model is the best fit model that indicates that the process is a type of monolayer sorption with the regression coefficients $R^2 \approx 1$. One of the characteristics of the Langmuir isotherm is the equilibrium parameter R_L. The value of R_L was found to be 0.229, i.e., $0 < R_L < 1$, which means that the sorption process of Nd(III) onto the MCh@GO nanocomposite is favorable, Table 1.

The Temkin isotherm assumes that a decrease in the heat of adsorption is linear and the adsorption is characterized by a uniform distribution of binding energies. It is expressed by the following eq 4

$$q_e = \ln(K_T C_e) \times RT/b \quad (4)$$

https://doi.org/10.1021/acsomega.4c04742
ACS Omega 2024, 9, 32175−32184

Table 2. Calculated Parameters of the Pseudo-First-Order, Pseudo-Second-Order, Intraparticle Diffusion, and Elovich Kinetic Models of Nd(III) onto the MCh@GO Nanocomposite

model	parameters	298 K	313 K	323 K	333 K
First-order kinetic	k_1 (min.$^{-1}$)	0.530	0.516	0.484	0.509
	q_e, calc. (mg/g)	31.844	35.285	40.554	43.690
	R^2	0.987	0.970	0.975	0.978
Second-order kinetic	k_2 (min.$^{-1}$)	0.022	0.019	0.015	0.015
	q_e, calc. (mg/g)	35.148	39.086	45.071	48.469
	R^2	0.913	0.893	0.907	0.909
	q_e, exp. (mg/g)	**31.45**	**34.5**	**39.75**	**42.95**
Intraparticle diffusion	k_{id} (mg g^{-1} min$^{-0.5}$)	7.20	6.74	5.77	5.10
	C	15.0	13.6	12.5	11.2
	R^2	0.532	0.545	0.517	0.529
Elovich	a(mg/min)	3.9	3.3	5.5	8.0
	b (g/mg^{-1})	0.105	0.082	0.076	0.071
	R^2	0.891	0.889	0.882	0.903

Table 3. Thermodynamic Parameters for the Sorption of Nd(III) onto the MCh@GO Nanocomposite

T, K°	$\Delta H°$ (kJ/mol)	$\Delta S°$(J/mol)	$\Delta G°$ (kJ/mol)
298	29.540	102.827	−1.308
313			−2.082
323			−3.639
333			−5.003

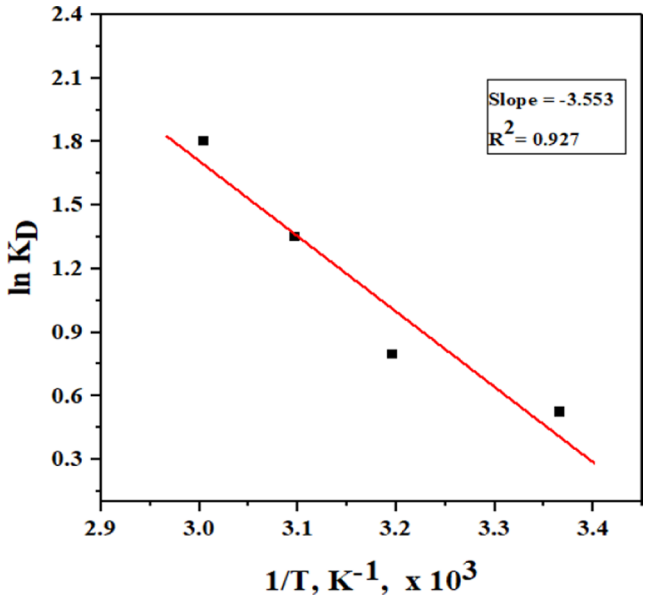

Figure 12. Effect of temperature on the adsorption of Nd(III) onto the MCh@GO nanocomposite (pH 4.5, V/m = 1000 mL/g, Nd(III)50 ppm).

where $b = RT/b$ is related to the heat of adsorption (J/mol), R is the gas constant (8314 J. mol^{-1}·K^{-1}), T is the absolute temperature (K), and K_T is the Temkin equilibrium constant (L/g) corresponding to the maximum binding energy. The Temkin constants are tabulated in Table 1.

3.2.4. Adsorption Kinetic Models. The sorption kinetics depends on the nature of both the sorbent material and sorbate species that affect the sorption process.[58,59] To explore the sorption mechanism, four kinetic models were used (first-order, second-order, intraparticle, and Elovich models). The pseudo-first-order mechanism equation is generally expressed as follows

$$q_t = q_e(1 - e^{-k_1 t}) \tag{5}$$

By plotting log q_t versus t, as represented in Figure 11a, straight lines were obtained. From the slopes and the intercepts, we can determine the pseudo-first-order rate constant, k_1, and the calculated adsorbed amounts at equilibrium, calc. q_e, as illustrated in Table 2.

The pseudo-second-order adsorption kinetic rate equation is defined as

$$q_t = \frac{K_2 q_e^2 t}{1 + K_2 q_e t} \tag{6}$$

where the values of the pseudo-second-order rate constant, k_2, and the amount adsorbed at equilibrium, q_e, can be evaluated as shown in Figure 11b and tabulated in Table 2. It is clear that the theoretical values of q_e are also closer to the experimental q_e values for the second-order kinetic model compared with those in the pseudo-first-order model. This suggests that the sorption process reaction of Nd(III) ions onto the MCh@GO nanocomposite follows the second-order kinetic model.

The intraparticle diffusion model can be evaluated from eq 7

$$q_t = K_i t^{1/2} + C \tag{7}$$

where k_i (mg g^{-1} min$^{-0.5}$) is the intraparticle diffusion rate constant and C refers to the boundary layer thickness and can be estimated from the plot of q_t and $t^{1/2}$. Figure 11c gives straight lines that do not pass through the origin; this indicates that the intraparticle diffusion is involved in the sorption process but not in the rate-controlling step due to the boundary layer effect. The values of k_i and C are listed in Table 2. It is worth mentioning that the value of k_i increased with temperature due to increasing mobility of the Nd(III).

The Elovich kinetic model emphasizes the activated chemisorptions and is expressed by eq 8

$$q_t = 1/\beta \ln(1 + \alpha\beta t) \tag{8}$$

where the constant (α) is known as the original adsorption rate (mg/g min) and (β) is a constant; they are illustrated in Table 3.

3.2.5. Effect of Temperature. The temperature has a great influence on the sorption process. Hence, the effect of temperature on the sorption of Nd(III) was investigated in the range of 298−333 K.

The thermodynamic parameters $\Delta H°$, $\Delta S°$, and $\Delta G°$ can be evaluated from the following equations

$$\ln K_D = \frac{\Delta S°}{R} - \frac{\Delta H°}{RT} \tag{9}$$

$$\Delta G° = \Delta H° - T\Delta S° \tag{10}$$

by drawing ln K_D against $1/T$, Figure 12, where the values of the above-mentioned thermodynamic parameters are tabulated in Table 3. The positive $\Delta H°$ value indicates the endothermic character of the process, and the negative value of $\Delta G°$ indicates that the process is spontaneous. The positive entropy change ($\Delta S°$) indicates that the adsorption of Nd(III) onto

https://doi.org/10.1021/acsomega.4c04742
ACS Omega 2024, 9, 32175−32184

Table 4. Comparison of Nd(III) Adsorption Capacity by Different Adsorbent Materials[49,60−68]

adsorbent	initial [Nd], mg/L	pH	equilibrium time	%R	Q_{max}, mg/g	refs
MCh@GO	50	4.5	5.0 min	62.90%	58.219	this study
functionalized Cr-MIL-101-PMIDA	100	5.5	360.0 min	90%	90.0	(60)
CA/P(P-T-A)/NZFO	30	5.5	50.0 min	96.73%	71.44	(61)
CS-MF	50	4.0	180.0 min	75.75%	44.29	(62)
CA@Fe_3O_4 NPs	5	7.0	30.0 min	90%	41.0	(63)
magnetic alginate (P_30_7) microcapsules	90	4.0	20.0 h	98%	45.5	(64)
magnetic iron oxide Fe_3O_4	10	8.22	120 min	99.90%	22.27	(65)
MPA-TEOS-ferrite	10	8.16	30.0 min	99.99%	25.58	(49)
cyphos@silica	200	4.0	180.0 min	67%	14.71	(66)
phosphorus-functionalized nanoporous carbon	500	6.1	1.0 h	67−68%	335.5	(67)
magnetic calcium alginate/carboxymethyl chitosan/$Ni_{0.2}Zn_{0.2}Fe_{2.6}O_4$	300	5.5	40 min	96%	73.4	(68)

the MCh@GO nanocomposite is accompanied with an increase in the randomness of the system as a result of increasing the rate of diffusion of the sorbate species across the external boundary layer.

3.3. Reusability. The regeneration and reuse of the adsorbent are vital criteria for assessing the commercial potential. In this respect, the loaded composite was regenerated using dilute hydrochloric acid (pH 1−2). The regeneration ratio was between 100 and 85% after 5.0 cycles. This result indicates that the positive charged amine groups in CS were protonated in acidic conditions, so the adsorbed Nd(III) ions left active bonding sites on the composite due to the electrostatic repulsion between the positive Nd(III) ions and adsorbent.

3.4. Comparison of Nd(III) Adsorption Capacity by Different Adsorbent Materials. Table 4 gives a comparison between different adsorbents and the investigated MCh@GO nanocomposite toward the sorption of Nd(III).[49,60−68] The results implied that the MCh@GO nanocomposite can be used efficiently for the remediation of Nd(III) from aqueous medium.

4. CONCLUSIONS

In summary, we have reported the synthesis and characterization of the magnetic chitosan/graphene oxide nanocomposite (MCh@GO) by FT-IR, XRD, SEM, and TGA that could be employed as an effective adsorbent for the removal of Nd(III) ions from aqueous media. Different factors affecting the sorption process such as pH, contact time, initial Nd(III) concentration, and temperature have been examined. It was found that the optimum conditions for the sorption of Nd(III) are at pH 4.5 within 5.0 min. The mechanism of the sorption process follows the pseudo-second order and obeys the Langmuir isotherm with a Q_{max} of 56.6 mg g^{-1}, being spontaneous and endothermic in nature. Moreover, the synthesized composite had a high reusability of up to five cycles of adsorption−regeneration that was achieved using relatively dilute hydrochloric acid. This ensures that this adsorbent is economical, eco-friendly, and promising for wastewater treatment. In the future work, the adsorption behavior of other lanthanides will be investigated.

AUTHOR INFORMATION

Corresponding Authors

Asmaa S. Al-salem − *Department of Nursing, Northern College of Nursing, Arar 73311, Saudi Arabia*; Email: Asmaa4767@gmail.com, asma@nec.edu.sa

AbdElAziz A. Nayl − *Department of Chemistry, College of Science, Jouf University, Sakaka, Aljouf 72341, Saudi Arabia*; orcid.org/0000-0003-0531-5194; Email: aanayel@ju.edu.sa, aanayl@yahoo.com

Authors

Mutairah S. Alshammari − *Department of Chemistry, College of Science, Jouf University, Sakaka, Aljouf 72341, Saudi Arabia*

Ismail M Ahmed − *Department of Chemistry, College of Science, Jouf University, Sakaka, Aljouf 72341, Saudi Arabia*

Complete contact information is available at: https://pubs.acs.org/10.1021/acsomega.4c04742

Author Contributions

All authors have contributed to this study at different stages. Conceptualization: A.S.A., A.A.N., I.M.A., and M.S.A.; methodology: A.S.A., I.M.A., and A.A.N.; software: A.S.A., I.M.A., A.A.N., and M.S.A.; validation: A.S.A., I.M.A., and A.A.N.; formal analysis: A.S.A.; I.M.A., and A.A.N.; investigation: A.S.A., I.M.A., and A.A.N.; writing—original draft preparation: A.S.A., A.A.N., I.M.A., and M.S.A; and writing—review and editing: A.S.A., A.A.N., I.M.A., and M.S.A. All authors have read and agreed to the published version of the article.

Notes

The authors declare no competing financial interest.

ACKNOWLEDGMENTS

A.S.A. extend her sincere thanks to the Northern College of Nursing for their cooperation with her.

REFERENCES

(1) Brião, G. d. V.; da Silva, M. G. C.; Vieira, M. G. A. Efficient and Selective Adsorption of Neodymium on Expanded Vermiculite. *Ind. Eng. Chem. Res.* **2021**, *60* (13), 4962−4974, DOI: 10.1021/acs.iecr.0c05979.

(2) Jowitt, S. M.; Werner, T. T.; Weng, Z.; Mudd, G. M. Recycling of the Rare Earth Elements. *Curr. Opin. Green Sustainable Chem.* **2018**, *13*, 1−7.

(3) El-Hefny, N. E.; Gasser, M. S.; Emam, S. S.; Mahmoud, W. H.; Aly, H. F. Comparative studies on Y(III) and Dy(III) extraction from hydrochloric and nitric acids by Cyanex 572 as a novel extractant. *J. Rare Earths* **2018**, *36* (12), 1342.

(4) Li, L.; Yu, B.; Davis, K.; King, A.; Dal-Cin, M.; Nicalek, A.; Du, N. Separation of Neodymium (III) and Lanthanum (III) via a Flat Sheet-Supported Liquid Membrane with Different Extractant-Acid Systems. *Membranes* **2022**, *12* (12), 1197−1212.

(5) Setyadji, M.; Suyanti. Extraction of Neodymium (III) from Neodymium Concentrate Using Synergistic Solvent D2EHPA, TOPO and TBP. *J. Phys.: Conf. Ser.* **2019**, *1198*, No. 032001.
(6) Riaño, S.; Foltova, S. S.; Binnemans, K. Separation of neodymium and dysprosium by solvent extraction using ionic liquids combined with neutral extractants: batch and mixer-settler experiments. *RSC Adv.* **2020**, *10*, 307−316.
(7) Ruiz, V. C. A.; Kuchi, R.; Parhi, P. K.; Lee, J. Y.; Jyothi, R. K. Environmentally friendly comprehensive hydrometallurgical method development for neodymium recovery from mixed rare earth aqueous solutions using organo phosphorus. *Sci. Rep.* **2020**, *10*, No. 16911.
(8) Allahkarami, E.; Rezai, B.; Bozorgmehr, M.; Adib, S. Extraction of neodymium(III) from aqueous solutions by solvent extraction with Cyanex 572. *Physicochem. Probl. Miner. Process.* **2021**, *57* (3), 127−135.
(9) Pramanik, B. K.; Shu, L.; Jegatheesan, J.; Shah, K.; Haque, N.; Bhuiyan, M. A. Rejection of rare earth elements from a simulated acid mine drainage using forward osmosis: The role of membrane orientation, solution pH, and temperature variation. *Process Saf. Environ. Prot.* **2019**, *126*, 53−59.
(10) Haritsah, I.; Adi, W. A.; Purwani, M. V.; Manaf, A. Improved separation of Ce, La, and Nd from a concentrate of rare-earth hydroxide via fractional precipitation. In: IOP conference series: materials science and engineering. *IOP Conf. Ser.: Mater. Sci. Eng.* **2019**, *496*, No. 012013.
(11) Song, G.; Wang, X.; Romero, C.; Chen, H.; Yao, Z.; Kaziunas, A.; Baltrusaitis, J.; et al. Extraction of selected rare earth elements from anthracite acid mine drainage using supercritical CO_2 via coagulation and complexation. *J. Rare Earths* **2021**, *39*, 83−89.
(12) Wu, X.; Feng, J.; Zhou, F.; Liu, C.; Chi, R. High sedimentation efficiency and enhanced rare earth recovery in the impurity removal process of rare earth leachate by flocculation system. *J. Environ. Chem. Eng.* **2024**, *12*, No. 112626.
(13) Hassas, B. V.; Rezaee, M.; Pisupati, S. V. Effect of various ligands on the selective precipitation of critical and rare earth elements from acid mine drainage. *Chemosphere* **2021**, *280*, No. 130684.
(14) Bashiri, A.; Nikzad, A.; Maleki, R.; Asadnia, M.; Razmjou, A. Rare Earth Elements Recovery Using Selective Membranes via Extraction and Rejection. *Membranes* **2022**, *12* (1), 80.
(15) Dong, Z.; Mattocks, J. A.; Deblonde, G. J. P.; Hu, D.; Jiao, Y.; Cotruvo, J. A.; Park, D. M. Bridging Hydrometallurgy and Biochemistry: A Protein-Based Process for Recovery and Separation of Rare Earth Elements. *ACS Cent. Sci.* **2021**, *7*, 1798−1808.
(16) Sakib, M. N.; Mallik, A. K.; Rahman, M. M. Update on chitosan-based electrospun nanofibers for wastewater treatment: A review. *Carbohydr. Polym. Technol. Appl.* **2021**, *2*, No. 100064.
(17) Sheth, Y.; Dharaskar, S.; Khalid, M.; Sonawane, S. An environment friendly approach for heavy metal removal from industrial wastewater using chitosan based biosorbent: A review. *Sustainable Energy Technol. Assess.* **2021**, *43*, No. 100951.
(18) Ahmad, S. Z. N.; SallehW, N. W.; Ismail, A. F.; Yusof, N.; Yusop, M. Z. M.; Aziz, F. Adsorptive removal of heavy metal ions using graphene-based nanomaterials: Toxicity, roles of functional groups and mechanisms. *Chemosphere* **2020**, *248*, No. 126008.
(19) Pena-Pereira, F.; Romero, V.; Calle, L. D. L.; Lavilla, I.; Bendicho, C. Graphene-based nanocomposites in analytical extraction processes. *Trends Anal. Chem.* **2021**, *142*, No. 116303.
(20) Sherlala, A. I. A.; Raman, A. A. A.; Bello, M. M.; Buthiyappan, A. Adsorption of arsenic using chitosan magnetic graphene oxide Nanocomposite. *J. Environ. Manage.* **2019**, *246*, 547−556.
(21) Maleki Dana, P.; Hallajzadeh, J.; Asemi, Z.; Mansournia, M. A.; Yousefi, B. Chitosan applications in studying and managing osteosarcoma. *Int. J. Biol. Macromol.* **2021**, *169*, 321−329.
(22) Demey, H.; Lapo, B.; Ruiz, M.; Fortuny, A.; Marchand, A.; Sastre, A. M. Neodymium Recovery by Chitosan/Iron(III) Hydroxide [ChiFer(III)] Sorbent Material: Batch and Column Systems. *Polymers* **2018**, *10* (2), 204.
(23) Di Virgilio, M.; Latorrata, S.; Cinzia Cristiani, C.; Dotelli, G. Analysis of the Adsorption-Release Isotherms of Pentaethylenehexamine-Modified Sorbents for Rare Earth Elements (Y, Nd, La). *Polymers* **2022**, *14* (23), 5063.
(24) Asadollahzadeh, M.; Torkaman, R.; M Mostaedi, T. Extraction and separation of rare earth elements by adsorption approaches: current status and future trends. *Sep. Purif. Rev.* **2021**, *50* (4), 417−444.
(25) Saha, D.; Bhasin, V.; Khalid, S.; et al. Adsorption of rare earth elements in carboxylated mesoporous carbon. *Sep. Purif. Technol.* **2023**, *314*, 123583−123593.
(26) Hermassi, M.; Granados, M.; C Valderrama, C.; et al. Recovery of rare earth elementsfrom acidic mine waters by integration of a selective chelating ion-exchanger anda solvent impregnated resin. *J. Environ. Chem. Eng.* **2021**, *9*, 105906−105920.
(27) Abu Elgoud, E. M.; Aly, M. I.; Hamed, M. M.; Nayl, A. A. NanoTafla nanocomposite as a novel low-cost and eco-friendly sorbent for strontium and europium ions. *ACS Omega* **2022**, *7*, 10447−10457.
(28) Zhao, F.; Repo, E.; Song, Y.; Yin, D.; Hammouda, S. B.; Chen, L.; Kalliola, S.; Tang, J.; Tam, K. C.; Sillanpää, M. Polyethylenimine-cross-linked cellulose nanocrystals for highly efficient recovery of rare earth elements from water and mechanism study. *Green Chem.* **2017**, *19*, 4816−4828.
(29) Lea, T.; Lea, V.; Dao, M.; Nguyen, Q.; Vu, T.; Nguyen, M.; Tran, D.; Le, H. Preparation of magnetic graphene oxide/chitosan composite beads for effective removal of heavy metals and dyes from aqueous solutions. *Chem. Eng. Commun.* **2019**, 1337−1352, DOI: 10.1080/00986445.2018.1558215.
(30) Lujanienė, G.; Novikau, R.; Joel, E. F.; Karaleviciute, K.; Šemcuk, S.; Mažeika, K.; Talaikis, M.; Pakštas, V.; Tumenas, S.; Mažeika, J.; Jokšas, K. Preparation of Graphene Oxide-Maghemite-Chitosan Composites for the Adsorption of Europium Ions from Aqueous Solutions. *Molecules* **2022**, *27* (22), 8035−8045.
(31) Ramezani, G.; Honarvar, B.; Emadi, M. Thermodynamic study of (Pb^{2+}) removal by adsorption onto modified magnetic Graphene Oxide with Chitosan and Cysteine. *J. Optoelectronical Nanostruct.* **2019**, *4* (3), 73−92.
(32) Zhuang, S.; Wang, J. Removal of Cobalt Ion from Aqueous Solution Using Magnetic Graphene Oxide/Chitosan Composite. *Environ. Prog. Sustainable Energy* **2019**, *38*, S32−S41.
(33) Abou El-Reash, Y. Magnetic Chitosan Modified with Cysteine-Glutaraldehyde as Adsorbent for Removal of Heavy Metals from Water. *J. Environ. Chem. Eng.* **2016**, *4* (4), 3835−3847.
(34) Liu, M.; Chen, C.; Hu, J.; Wu, X.; Wang, X. Synthesis of magnetite/graphene oxide composite and application for cobalt(II) removal. *J. Phys. Chem. C* **2011**, *115* (51), 25234−25240.
(35) Lian, Z.; Li, Y.; Xian, H.; Ouyang, X-k.; Lu, Y.; Peng, X.; Hu, D. EDTA-functionalized magnetic chitosan oligosaccharide and carboxymethyl cellulose nanocomposite: Synthesis, characterization, and Pb(II) adsorption performance. *Int. J. Biol. Macromol.* **2020**, *165*, 591−600.
(36) Anush, S. M.; Chandan, H. R.; Gayathri, B. H.; Manju, N.; Vishalakshi, B.; Kalluraya, B. Graphene oxide functionalized chitosan-magnetite nanocomposite for removal of Cu(II) and Cr(VI) from waste water. *Int. J. Biol. Macromol.* **2020**, *164*, 4391−4402.
(37) Marczenko, Z. *Specrtophotometric Determination of Elements*; Johon Wiley and sons, Inc.: New York*1986*, pp 438−443 DOI: 10.1021/ja025282c.
(38) Freire, J. M. A.; Moreira, Í. O.; de M França, A. M.; da Silva, L. T. V.; dos Santos, L. P. M.; Santos Medeiros, S. L.; de Vasconcelos, I. F.; Loiola, A. R.; Antunes, R. A.; do Nascimento, R. F.; Longhinotti, E. Functionalized magnetic graphene oxide composites for selective toxic metal adsorption. *Environ. Nanotechnol., Monit. Manage.* **2023**, *20*, No. 100843, DOI: 10.1016/j.enmm.2023.100843.
(39) Pal, K.; Bharti, D.; Sarkar, P.; Anis, A.; Kim, D.; Chałas, R.; Maksymiuk, P.; Stachurski, P.; Jarzębski, M. Selected Applications of Chitosan Composites. *Int. J. Mol. Sci.* **2021**, *22* (20), 10968.

(40) Dreyer, D. R.; Ruoff, R. S.; Bielawski, C. W. From Conception to Realization: an Historial Account of Graphene and Some Perspectives for its Future. *Angew. Chem., Int. Ed.* **2010**, *49* (49), 9336−9344.
(41) Yan, D.; Yanzhen, L.; Yinling, L.; Na, L.; Xue, Z.; Chen, Y. Antimicrobial Properties of Chitosan and Chitosan Derivatives in the Treatment of Enteric Infections. *Molecules* **2021**, *26* (23), 7136−7148.
(42) Kloster, G. A.; Valiente, M.; Marcovich, N. E.; Mosiewicki, M. A. Adsorption of arsenic onto films based on chitosan and chitosan/nano-iron oxide. *Int. J. Biol. Macromol.* **2020**, *165*, 1286−1295.
(43) Subedi, N.; Lähde, A.; Abu-Danso, E.; Iqbal, J.; Bhatnagar, A. A comparative study of magnetic chitosan (Chi@Fe_3O_4) and grapheme oxide modified magnetic chitosan (Chi@Fe_3O_4GO) nanocomposites for efficient removal of Cr(VI) from water. *Int. J. Biol. Macromol.* **2019**, *137*, 948−959.
(44) Samuel, M. S.; Bhattacharya, J.; Raj, S.; Santhanam, N.; Singh, H.; Singh, N. D. P. Efficient removal of Chromium(VI) from aqueous solution using chitosan grafted graphene oxide (CS-GO) nanocomposite. *Int. J. Biol. Macromol.* **2019**, *121*, 285−292.
(45) Nayl, A. A.; Abd-Elhamid, A. I.; Arafa, W. A.; Ahmed, I. M.; El-Shanshory, A. A.; Abu-Saied, M. A.; Soliman, H. M. A.; Abdelgawad, M. A.; Ali, H. M.; Bräse, S. ChitosanFunctionalized-Graphene Oxide (GO@CS) Beads as an Effective Adsorbent to Remove Cationic Dye from Wastewater. *Polymers* **2022**, *14* (19), 4236−4248.
(46) Arunachalam, K. D. Bio-adsorption of methylene blue dye using chitosan- extracted from Fenneropenaeus indicus shrimp shell waste. *J. Aquacult. Mar. Biol.* **2021**, *10*, 146−150.
(47) Shan, H.; Zeng, C.; Zhao, C.; Zhan, H. Iron oxides decorated graphene oxide/chitosan composite beads for enhanced Cr(VI) removal from aqueous solution. *Int. J. Biol. Macromol.* **2021**, *172*, 197−209.
(48) Liu, M.; Zhang, X.; Li, Z.; Qu, L.; Han, R. Fabrication of zirconium (IV)-loaded chitosan/Fe_3O_4/graphene oxide for efficient removal of alizarin red from aqueous solution. *Carbohydr. Polym.* **2020**, *248*, No. 116792.
(49) Tu, Y.-J.; You, C.-F.; Lo, S.-C.; Chan, T.-S.; Chung, C.-H. Recycling of Neodymium Enhanced by Functionalized Magnetic Ferrite. *Environ. Technol.* **2019**, *40*, 1592−1604, DOI: 10.1080/09593330.2018.1426643.
(50) Rebekah, A.; Navadeepthy, D.; Bharath, G.; Viswanathan, C.; Ponpandian, N. Removal of 1-napthylamine using magnetic graphene and magnetic graphene oxide functionalized with Chitosan. *Environ. Nanotechnol., Monit. Manage.* **2021**, *15*, 100450−100460.
(51) Li, Y.; Dong, X.; Zhao, L. Application of magnetic chitosan nanocomposites modified by graphene oxide and polyethyleneimine for removal of toxic heavy metals and dyes from water. *Int. J. Biol. Macromol.* **2021**, *192*, 118−125.
(52) Neves, T. D. F.; Dalarme, N. B.; Silva, P. M. M. D.; Landers, R.; Picone, C. S. F.; Prediger, P. Novel magnetic chitosan/quaternary ammonium salt graphene oxide composite applied to dye removal. *J. Environ. Chem. Eng.* **2020**, *8*, No. 103820.
(53) Cao, L.; Zhang, F.; Wang, Q.; Wu, X. Fabrication of chitosan/graphene oxide polymer nanofiber and its biocompatibility for cartilage tissue engineering. *Mater. Sci. Eng. C* **2017**, *79*, 697−701.
(54) Zhang, L.; Wu, D.; Zhu, B.; Yang, Y.; Wang, L. Adsorption and selective separation of neodymium with magnetic alginate microcapsules containing the extractant 2-ethylhexyl phosphonic acid mono-2-ethylhexyl ester. *J. Chem. Eng. Data* **2011**, *56*, 2280−2289.
(55) Puigdomenech, I. HYDRA (Hydrochemical Equilibrium Constant Database) and MEDUSA (Make Equilibrium Diagrams Using Sophisticated Algorithms) Programs. Royal Institute of Technology: Sweden, 2013 http://www.ke-mi.kth.se/medusa.
(56) Saravanan, A.; Sundararaman, T. R.; Jeevanantham, S.; Karishma, S.; Kumar, P. S.; Yaashikaa, P. R. Effective adsorption of Cu(II) ions on sustainable adsorbent derived from mixed biomass (Aspergillus campestris and agro waste): Optimization, isotherm and kinetics study. *Groundwater Sustainable Dev.* **2020**, *11*, No. 100460.
(57) Ahmed, I. M.; Nayl, A. A. A novel adsorbent functionalized with tri-octylamine (TOA) to effective removal of Cr(VI) from sulfate medium. *J. Taiwan Inst. Chem. Eng.* **2021**, *121*, 292−301.
(58) Hamed, M. M.; Holiel, M.; Ahmed, I. M. Sorption Behavior of Cesium, Cobalt and Europium Radionuclides onto Hydroxyl Magnesium Silicate. *Radiochim. Acta* **2016**, *104* (12), 873−890.
(59) Deng, H.; Li, X.; Huang, Y.; Ma, X.; Wu, L.; Cheng, T. An efficient composite ion exchanger of silica matrix impregnated with ammonium molybdophosphate for cesium uptake from aqueous solution. *Chem. Eng. J.* **2016**, *286*, 25−35.
(60) Lee, Y. R.; Yu, K.; Ravi, S.; Ahn, W. S. Selective Adsorption of Rare Earth Elements over Functionalized Cr-MIL-101. *ACS Appl. Mater. Interfaces* **2018**, *10* (28), 23918−23927.
(61) Javadian, H.; Ruiz, M.; Taghvai, M.; Sastre, A. M. Novel magnetic nanocomposite of calcium alginate carrying poly-(pyrimidine-thiophene-amide) as a novel green synthesized polyamide for adsorption study of neodymium, terbium, and dysprosium rare-earth ions. *Colloids Surf., A* **2020**, *603*, No. 125252.
(62) Durán, S. V.; Lapo, B.; Meneses, M.; Sastre, A. M. Recovery of neodymium (III) from aqueous phase by chitosan-manganese-ferrite magnetic beads. *Nanomaterials* **2020**, *10* (6), No. 1204.
(63) Ashour, R. M.; El-sayed, R.; Abdel-Magied, A. F.; Abdel-khalek, A. A.; Ali, M. M.; Forsberg, K.; Uheida, A.; Muhammed, M.; Dutta, J. Selective separation of rare earth ions from aqueous solution using functionalized magnetite nanoparticles: kinetic and thermodynamic studies. *Chem. Eng. J.* **2017**, *327*, 286−296.
(64) Zhang, B.; Hu, R.; Sun, D.; Wu, T.; jiang, Y. Fabrication of chitosan/magnetitegraphene oxide composites as a novel bioadsorbent for adsorption and detoxifcation of Cr(VI) from aqueous solution. *Sci. Rep.* **2018**, *8*, No. 15397.
(65) Tu, Y.-J.; Lo, S.-C.; You, C.-F. Selective and fast recovery of neodymium from seawater by magnetic iron oxide Fe_3O_4. *Chem. Eng. J.* **2015**, *262* (2015), 966−972, DOI: 10.1016/j.cej.2014.10.025.
(66) Mohamed, W. R.; Metwally, S. S.; Ibrahim, H. A.; El-Sherief, E. A.; Mekhamer, H. S.; Moustafa, I. M. I.; Mabrouk, E. M. Impregnation of task-specific ionic liquid into a solid support for removal of neodymium and gadolinium ions from aqueous solution. *J. Mol. Liq.* **2017**, *236*, 9−17.
(67) Saha, D.; Akkoyunlu, S. D.; Thorpe, R.; Hensley, D. K.; Chen, J. Adsorptive recovery of neodymium and dysprosium in phosphorous functionalized nanoporous carbon. *J. Environ. Chem. Eng.* **2017**, *5* (5), 4684−4692.
(68) Javadian, H.; Ruiz, M.; Saleh, T. A.; Sastre, A. M. Ca-alginate/carboxymethyl chitosan/$Ni_{0.2}Zn_{0.2}Fe_{2.6}O_4$ magnetic bionanocomposite: Synthesis, characterization and application for single adsorption of Nd^{+3}, Tb^{+3}, and Dy^{+3} rare earth elements from aqueous media. *J. Mol. Liq.* **2020**, *306*, 112760−112771.

https://doi.org/10.1021/acsomega.4c04742
ACS Omega 2024, 9, 32175−32184